JOURNAL OF THERMOPHYSICS AND HEAT TRANSFER
Vol. 21, No. 3, July–September 2007

Technical Notes

TECHNICAL NOTES are short manuscripts describing new developments or important results of a preliminary nature. These Notes should not exceed 2500 words (where a figure or table counts as 200 words). Following informal review by the Editors, they may be published within a few months of the date of receipt. Style requirements are the same as for regular contributions (see inside back cover).

Rotational Effects on Pressure Drop in Smooth and Ribbed Two-Pass Ducts

Kyung Min Kim,* Dong Hyun Lee,* and Hyung Hee Cho†
Yonsei University, Seoul 120-749, Republic of Korea

DOI: 10.2514/1.27538

Nomenclature

C_p = nondimensional pressure-drop coefficient
D_h = duct hydraulic diameter, m
D_{naph} = mass diffusion coefficient of naphthalene vapor in air, $\text{m}^2 \cdot \text{s}^{-1}$
e = rib height, m
f = friction factor
f_0 = friction factor of a fully developed turbulent flow in a smooth pipe
H = passage height, m
h_m = mass transfer coefficient, $\text{m} \cdot \text{s}^{-1}$
P_{ref} = reference pressure
P_x = local pressure
p = rib-to-rib pitch
Re = Reynolds number, $D_h u_b/\nu$
Ro = rotation number, $D_h\Omega/u_b$
Sc = Schmidt number of naphthalene in air
Sh = Sherwood number, $h_m D_h/D_{\text{naph}}$
Sh_0 = Sherwood number of a fully developed turbulent flow in a smooth pipe, $0.023Re^{0.8}Sc^{0.4}$
$\overline{Sh}$ = regional-averaged Sherwood number
u_b = mean flow velocity, $\text{m} \cdot \text{s}^{-1}$
W = width of the passage, m
w = rib width, m
x = streamwise distance from the rotating axis
y = lateral distance from the center of the channel
z = distance from the center toward the vertical direction
η = thermal performance
ν = kinematic viscosity
ρ = density of the fluid
Ω = angular velocity

I. Introduction

IN THIS Technical Note, we will experimentally investigate pressure-drop characteristics in coolant passages of a rotating gas turbine blade. The internal cooling passages usually have angled-rib turbulators installed. It results in significant enhancement of heat transfer in coolant passages. Consequently, many groups [1–6] dealt with heat transfer, fluid flow, and pressure-drop characteristics in the case of stationary ducts with angled ribs (or, mostly, heat transfer characteristics in rotating ducts). However, to design the internal cooling passages of gas turbine blades, the pressure drop and thermal performance should be examined under rotating conditions. Therefore, the objective of this Note is to illustrate the pressure coefficient distributions in the ducts with various rotation numbers and rib arrangements. The pressure coefficients in the present study and the mass transfer coefficients in the previous studies [7,8] induce thermal performance that should be considered in the design of an internal passage.

Received 16 November 2006; accepted for publication 4 April 2007.

*Graduate Student, Department of Mechanical Engineering.
†Professor, Department of Mechanical Engineering; hhcho@yonsei.ac.kr (Corresponding Author).

II. Experimental Apparatus and Procedures

A. Rotating Facility and Test Section

The experimental apparatus and procedure are the same as those described in Kim et al. [7,8]. Present experiments are conducted with a fixed Reynolds number of 10,000 and three rotation numbers of 0.0, 0.1, and 0.2. In the test, the rotation number of 0.2 corresponds to approximately 420 rpm.

The schematics of the test ducts with smooth, cross-ribbed, and parallel-ribbed walls are shown in Fig. 1. The present experimental apparatus has the duct aspect ratio W/H of 0.5 (20 mm/40 mm), the hydraulic diameter of 26.67 mm, and the ratio of divider wall thickness to the hydraulic diameter of 0.375. As shown in Fig. 1a, the streamwise, lateral, and vertical direction corresponds to the x, y, and z axes, respectively. The rib turbulators installed in the duct have a rib angle-of-attack of 70 deg with respect to the main duct flow direction and are attached to the leading and trailing surfaces in cross- (Fig. 1b) and parallel-rib (Fig. 1c) arrangements. The rib cross section is 2 mm (e) × 3 mm (w) and the rib-to-rib pitch p is 7.5 times of the rib height e. Pressure taps with a hole diameter of 0.8 mm are drilled at each centerline on the side, leading, and trailing surfaces to measure the pressure coefficients through the channel, as shown in Fig. 2. A pressure sensor unit (miniature electronic pressure scanners consisting of an array of silicon piezoresistive pressure sensors) is used to measure the pressure differences between each tap and the reference tap at $x = -12.37$ on the side wall in the first pass.

B. Data Reduction

The local pressure coefficients on the leading and trailing surfaces are nondimensionalized by normalizing with the velocity and density of the main flow as

$$C_p = (P_x - P_{\text{ref}})/[(1/2)\rho u_b^2] \tag{1}$$

The regional pressure drop is obtained from the slope calculated by a linear curve-fitting of the local pressure-difference data on the side wall in each region (the first pass is $-12.37 \le x/D_h \le -2.25$, the turning region is $-2.25 \le x/D_h \le 2.25$, the upstream part of the second pass is $2.25 \le x/D_h \le 5.62$, and the downstream part of the second pass is $5.62 \le x/D_h \le 12.37$) of the channel $\Delta P/\Delta L$ in which the static pressure decreases linearly. The friction factor is calculated with the average pressure drop on the side wall as

$$f = \Delta P/[4(\Delta L/D_h)(1/2)\rho u_b^2] \tag{2}$$

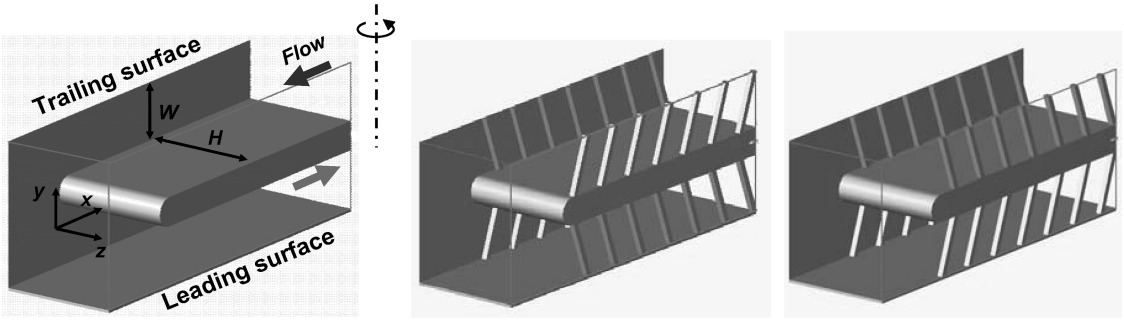

a) Smooth duct b) Cross-ribbed duct c) Parallel-ribbed duct

Fig. 1 Geometry of the ducts.

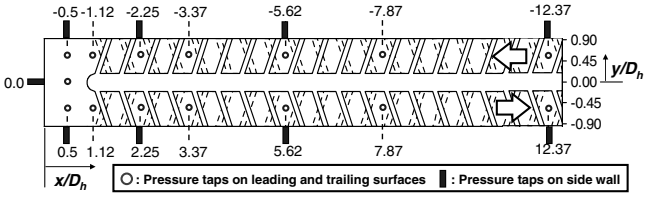

Fig. 2 Location of pressure taps (e.g., cross-ribbed duct).

The uncertainty of the friction factor is estimated to be within $\pm 4.7\%$ at a 95% confidence level by using the uncertainty estimation method of Kline and McClintock [9]. The pressure-drop results are presented as the friction factor ratios f/f_0, where f_0 represents the friction factor for a fully developed turbulent flow in a stationary smooth circular tube. The empirical equation that closely fits the Kármán–Nikuradse equation proposed by Petukhov [10] is employed, as $f_0 = 2(2.236\ln Re - 4.639)^{-2}$.

The thermal performance η, obtained by considering both the heat/mass transfer augmentation and the friction loss, is presented based on the constant-pumping-power condition and it is expressed as the following equation:

$$\eta = (\overline{Sh}/Sh_0)/(f/f_0)^{1/3} \tag{3}$$

where $\overline{Sh}/Sh_0$ is the regional-averaged Sherwood number ratio for each region. These heat/mass transfer data are obtained by the experimental results of Kim et al. [7,8].

III. Results and Discussion

Figure 3 presents the local pressure coefficient distributions at each location on the leading and trailing surfaces of the smooth, cross-ribbed, and parallel-ribbed ducts. With the increment of the rotation number, the local pressure coefficients in the smooth case increase on the trailing surface of the first pass, but decrease on the leading surface of the first pass and on the trailing surface of the second pass. In particular, the values are not changed on the leading surface of the second pass. As reported by Kim et al. [7], it is because the separation bubble induced by duct curvature disappears quickly in the second pass of the smooth duct with the increment of the rotation number. In the cross-ribbed case, the pressure coefficients also increase on the trailing surface of the first pass and on the leading surface of the second pass. However, the values decrease on the leading surface of the first pass and on the trailing surface of the second pass. This is because the separation bubble soon disappears after the turning region. In the parallel-ribbed case, the pressure coefficients increase on the trailing surface of the first pass and on the leading surface of the second pass. However, the values decrease on the leading surface of the first pass and are almost the same on the trailing surface of the second pass. The reason for having similar values is that the rotating direction of the secondary flow by the angled ribs is different from that of both the duct rotation and turning region. Therefore, the secondary flow becomes much weaker near the trailing surface of the second pass.

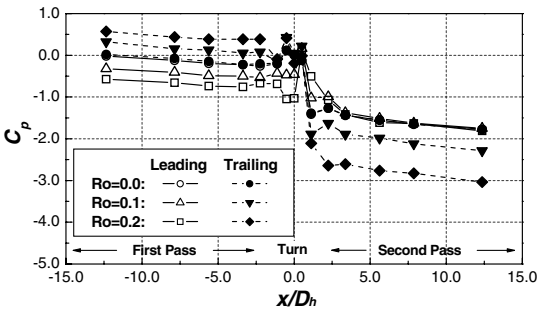

a) Smooth duct

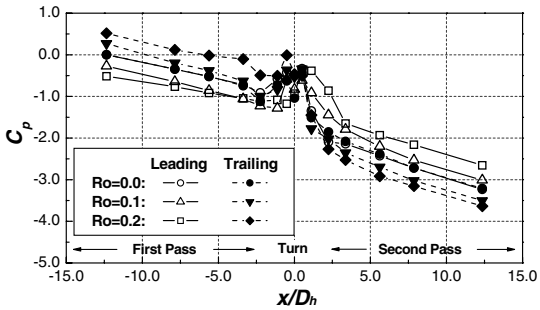

b) Cross-ribbed duct

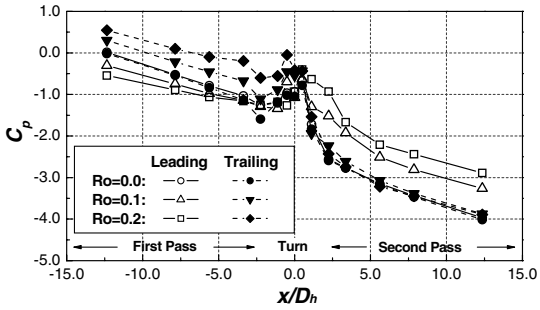

c) Parallel-ribbed duct

Fig. 3 Pressure coefficient distributions at various rotation numbers.

For each duct, although the slope of the pressure coefficients is dissimilar due to the different number of vortices produced by the angled ribs, the spacing in pressure between the leading and trailing surfaces are constant under the same rotation-number condition. It is noted that the effects of the Coriolis force are significant compared with both the inertia of the relative motion and viscous action, and the difference of pressure by the Coriolis force is also a function of flow velocity and angular velocity, as mentioned by Tritton [11].

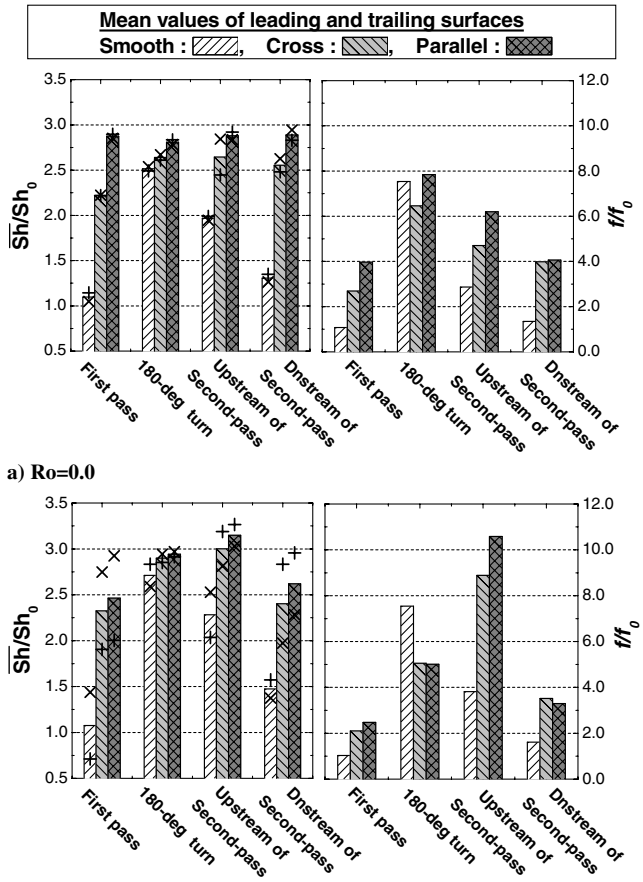

Fig. 4 Mean Sherwood number on leading (+) and trailing (×) surfaces and friction factor ratios at each region.

Figure 4 displays the regional-averaged values of the Sherwood numbers obtained by Kim et al. [7,8] and the results of the pressure-drop experiments in the form of the friction factor ratios f/f_0 for the stationary ($Ro = 0.0$) and rotating ($Ro = 0.2$) cases at $Re = 10,000$.

As shown in the left side of Fig. 4a (stationary ducts), the regional-averaged Sherwood number ratios $\overline{Sh}/Sh_0$ on the leading (+) and trailing (×) surfaces are almost the same in the first pass of all ducts, but are dissimilar after the turning region in only cross-ribbed ducts, because of asymmetric secondary flow induced by the cross-ribbed arrangement in the first pass. In all tested ducts, the highest values appear in the parallel-ribbed case, due to the strong secondary flow. In each region of the smooth duct, the heat/mass transfer is the highest in the turning region and then the value decreases gradually after the turning region. In the ribbed ducts, however, the Sherwood number ratios are high in all of the regions, because the heat/mass transfer is enhanced by the angled-rib turbulators as well as the duct turning.

In the rotating cases (Fig. 4b), the mean values have a large discrepancy between the leading and trailing surfaces due to the Coriolis force. In general, the values in the first pass are higher on the trailing surface in the case of outward flow, but reverse in the second pass in the case of inward flow. The mean values in the two ribbed ducts are the highest in the upstream part of the second pass, but in the turning region in only the smooth duct. This is because the secondary flow is additionally strengthened by the angled-rib turbulators.

The right side of Fig. 4 depicts friction losses in each region for the different rib arrangements. In the stationary cases (Fig. 4a), the highest friction loss appears in the parallel-ribbed duct among all of the ducts and in the turning region among all of the regions, due to the strong vortices by rib turbulators and the turning region. In the rotating cases (Fig. 4b), except the case with the smooth walls, the highest friction loss appears in the upstream part of the second pass.

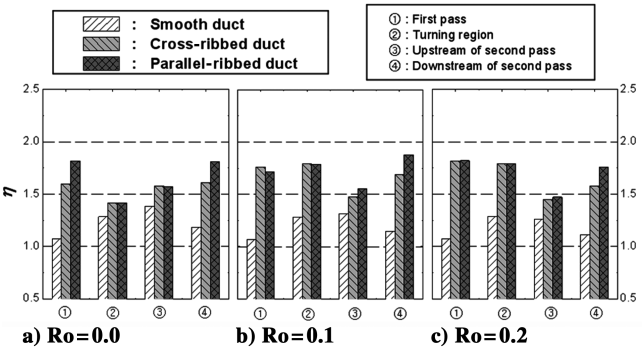

Fig. 5 Thermal performance at each region.

The reason is that one large asymmetric secondary flow generated after the turning region is disturbed by the angled-rib turbulators, as mentioned by Kim et al. [7,8]. Furthermore, the friction factor is the highest in the parallel-ribbed duct because the parallel-rib arrangement generates strong secondary flow and many vortices.

Figure 5 shows thermal performance in each region with the smooth, cross-ribbed, and parallel-ribbed walls in the stationary and rotating cases. It is estimated under the constant-pumping-power condition, as presented in Eq. (3). In the stationary cases (Fig. 5a), the thermal performance is the lowest in the turning region of two ribbed ducts, but in the first pass of only the smooth duct. For the rib arrangements, the thermal performance with the cross ribs and parallel ribs is about 1.5 and 1.7 times higher than that with the smooth walls in the first pass and the downstream part of the second pass, respectively. However, two ribbed cases are almost the same in the turning region and the upstream part of the second pass, because the duct turning affects the dominant force in these regions.

In the rotating cases (Figs. 5b and 5c), in both ribbed ducts, the lowest value appears in the upstream part of the second pass. The values are all higher and less similar in all of the regions except the downstream region of the second pass. It is noted that the difference of the thermal performance is not great for the rib arrangements in the rotating duct, even though the heat/mass transfer and pressure drop have the differences in the local region. In the downstream part of the second pass, the thermal performance in the cross-ribbed case is low, because the high friction loss by the turning region is maintained until the downstream part of the second pass.

IV. Conclusions

In the present study, the pressure drop and thermal performance characteristics of the internal cooling passages with various rotation numbers ($Ro = 0.0$, 0.1 and 0.2) and rib arrangements with a rib angle-of-attack of 70 deg at $Re = 10,000$ were investigated. From the experimental results, the following conclusions were drawn.

As the rotation number increased, in general, the pressure coefficients increased on the trailing surface of the first pass and on the leading surface of the second pass. In contrary, the values decreased on the leading surface of the first pass. However, on the trailing surface of the second pass, the pressure coefficient decreased only in the cross-ribbed duct, but stayed constant in the smooth and parallel-ribbed ducts, because of the different separation bubble or the secondary flow induced by the rib turbulators, duct rotation, and turning region. At the same rotation number, the difference in pressure between the leading and trailing surfaces was constant. The highest friction loss among all of the regions appeared in the turning region of the stationary ducts and only the rotating duct with the smooth walls, but appeared in the upstream part of the second pass of the rotating ribbed ducts. For the cross- and parallel-rib arrangements, the heat/mass transfer and pressure drop were different locally. However, the differences of the thermal performance were not significant for the rib arrangements in the rotating cases and the values were higher than those in the smooth case.

Acknowledgments

This work was supported partially by the Electric Power Industry Technology Evaluation and Planning program.

References

[1] Taslim, M. E., Li, T., and Kercher, D. M., "Experimental Heat Transfer and Friction in Channels Roughened with Angled, V-Shaped, and Discrete Ribs on Two Opposite Walls," *Journal of Turbomachinery*, Vol. 118, No. 1, 1996, pp. 20–28.

[2] Chyu, M. K., "Regional Heat Transfer in Two-Pass and Three-Pass Passages with 180-Deg Sharp Turns," *Journal of Heat Transfer*, Vol. 113, No. 1, 1996, pp. 63–70.

[3] Mokizuchi, S., Murata, A., Shibata, R., and Yang, W. J., "Detailed Measurements of Local Heat Transfer Coefficients in Turbulent Flow Through Smooth and Rib-Roughened Serpentine Passages with a 180° Sharp Bend," *International Journal of Heat and Mass Transfer*, Vol. 42, No. 11, 1999, pp. 1925–1934.

[4] Iacovides, H., Jackson, D. C., Ji, H., Kelemenis, G., Launder, B. E., and Nikas, K., "LDA Study of the Flow Development Through an Orthogonally Rotating U-Bend of Strong Curvature and Rib-Roughened Walls," *Journal of Turbomachinery*, Vol. 120, No. 2, 1998, pp. 386–391.

[5] Azad, G. S., Uddin, H. J., Han, J. C., Moon, H. K., and Glezer, B., "Heat Transfer in a Two-Pass Rectangular Rotating Channel with 45° Angled Rib Turbulators," *Journal of Turbomachinery*, Vol. 124, No. 2, 2002, pp. 251–259.

[6] Liou, T.-M., Chen, M.-Y., and Wang, Y.-M., "Heat Transfer, Fluid Low and Pressure Measurements Inside a Rotating Two-Pass Duct with Detached 90° Ribs," *Journal of Turbomachinery*, Vol. 125, No. 3, 2003, pp. 565–574.

[7] Kim, K. M., Kim, Y. Y., Lee, D. H., Rhee, D. H., and Cho, H. H., "Local Heat/Mass Transfer Phenomena in Rotating Passage, Part 1: Smooth Passage," *Journal of Thermophysics and Heat Transfer*, Vol. 20, No. 2, 2006, pp. 188–198.

[8] Kim, K. M., Kim, Y. Y., Lee, D. H., Rhee, D. H., and Cho, H. H., "Local Heat/Mass Transfer Phenomena in Rotating Passage, Part 2: Angled Ribbed Passage," *Journal of Thermophysics and Heat Transfer*, Vol. 20, No. 2, 2006, pp. 199–210.

[9] Kline, S. J., and McClintock, F. A., "Describing Uncertainty in Single-Sample Experiments," *Mechanical Engineering*, Vol. 75, Jan. 1953, pp. 3–8.

[10] Petukhov, B. S., "Heat Transfer and Friction in Turbulent Pipe Flow with Various Physical Properties," *Advances in Heat Transfer*, Vol. 6, Academic Press, New York, 1970, pp. 503–564.

[11] Tritton, D. J., "Flow in Rotating Fluids," *Physical Fluid Dynamics*, 2nd ed., Clarendon, Oxford, 1988, pp. 215–242.